Optimal design study of thermoacoustic regenerator with lexicographic optimization method

L.K. Tartibu
Department of Mechanical Engineering, Mangosuthu University of Technology, Durban, South Africa, and
B. Sun and M.A.E. Kaunda
Department of Mechanical Engineering, Cape Peninsula University of Technology, Cape Town, South Africa

Received 11 September 2012
Revised 26 July 2013
Accepted 2 September 2013

Abstract

Purpose – This paper aims to illustrate the use of the augmented epsilon-constraint method implemented in general algebraic modelling system (GAMS), aimed at optimizing the geometry of a thermoacoustic regenerator. Thermoacoustic heat engines provide a practical solution to the problem of heat management where heat can be pumped or spot cooling can be produced. However, the most inhibiting characteristic of thermoacoustic cooling is their current lack of efficiencies.

Design/methodology/approach – Lexicographic optimization is presented as an alternative optimization technique to the common used weighting methods. This approach establishes a hierarchical order among all the optimization objectives instead of giving them a specific (and most of the time, arbitrary) weight.

Findings – A practical example is given, in a hypothetical scenario, showing how the proposed optimization technique may help thermoacoustic regenerator designers to identify Pareto optimal solutions when dealing with geometric parameters. This study highlights the fact that the geometrical parameters are interdependent, which support the use of a multi-objective approach for optimization in thermoacoustic.

Originality/value – The research output from this paper can be a valuable resource to support designers in building efficient thermoacoustic device. The research illustrates the use of a lexicographic optimization to provide more meaningful results describing the geometry of thermoacoustic regenerator. It applies the epsilon-constraint method (AUGMENCON) to solve a five-criteria mixed integer non-linear problem implemented in GAMS (GAM software).

Keywords Design, Implementing, Managing and practicing innovation, Optimization algorithms, Mechanical design, Modelling, Multi-objective/attribute decision-making, Design strategies

Paper type Research paper

1. Introduction

This work illustrates the use of lexicographic optimization and demonstrates how multi-objective optimization approach can be used to optimize the design and

This research was supported by the Department of Mechanical Engineering at Cape Peninsula University of Technology, Cape Town, South Africa.

Journal of Engineering, Design and Technology
Vol. 13 No. 3, 2015
pp. 499-519

1726-0531
DOI 10.1108/JEDT-09-2012-0039

performance of thermoacoustic devices. Thermoacoustics combines the branches of acoustics and thermodynamics together to move heat by using sound. While acoustics is primarily concerned with the macroscopic effects of sound transfer like coupled pressure and motion oscillations, thermoacoustics focusses on the microscopic temperature oscillations that accompany these pressure changes. Thermoacoustics takes advantage of these pressure oscillations to move heat on a macroscopic level. This results in a large temperature difference ΔT between the hot and cold sides of a solid material and causes refrigeration (Swift, 1988).

In the process, the solid material acts as a regenerator (or stack). When a temperature difference is applied across this regenerator and a sound wave passes through the regenerator from the cold to the hot side, a parcel of gas executes a thermoacoustic cycle. The gas will subsequently be compressed, displaced and heated, expanded, displaced again and cooled (Figure 1). During this cycle, the gas is being compressed at low temperature, while expansion takes place at high temperature. This means that work is performed on the gas. The basic mechanics behind thermoacoustics are already well understood. A detailed explanation of the way thermoacoustic coolers work is given by Swift (1988) and Wheatley *et al.* (1985).

Figure 2 shows a very simple prototypical standing wave, quarter-wavelength thermoacoustic engine. The closed end of the resonance tube is the velocity node and the pressure antinode. The porous stack is located near the closed end, and the interior gas experiences large pressure oscillations and relatively small displacement. Heat input is provided by a heating wire, causing a temperature gradient to be established across the stack (in the axial direction). A gas in the vicinity of the walls inside the regenerative unit experiences compression, expansion and displacement when it is subject to a sound wave. Over the course of the cycle, heat is added to the gas at high pressure, and heat is withdrawn from it at low pressure. This energy imbalance results in an increase of the

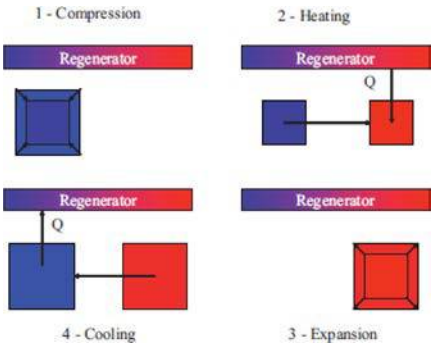

Figure 1.
Sequence of process steps in regenerator

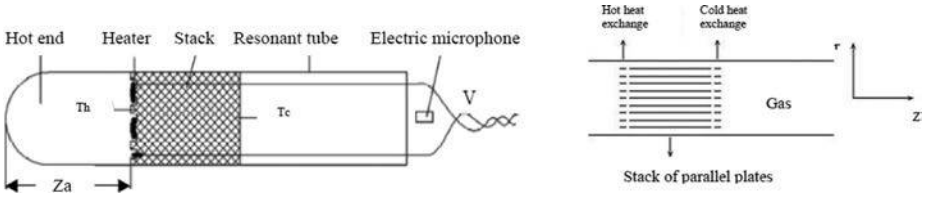

Figure 2.
Prototype of a small-scale thermoacoustic engine or prime mover

pressure amplitude from one cycle to the next, until the acoustic dissipation of the sound energy equals the addition of heat to the system (Swift *et al.*, 2000; Bastyr and Keolian, 2003; Poese *et al.*, 2004; Backhaus and Swift, 2000). Research is therefore focussing on optimizing the modelling approach, so that thermoacoustic coolers can compete with commercial refrigerators.

Optimization techniques as a design supplement have been under-utilized prior to Zink *et al.* (2009) and Trapp *et al.* (2011) studies. Some existing efforts include Minner *et al.* (1997), Wetzel and Herman (1997), Besnoin (2001) and Tijani *et al.* (2002) studies. A common trait of all these studies is the utilization of a linear approach while trying to optimize the device. Additionally, most studies [the exception being the Minner *et al.* (1997) study] have been limited to parametric studies to estimate the effect of single design parameters on device performance and ignored thermal losses to the surroundings. These parametric studies are unable to capture the nonlinear interactions inherent in thermoacoustic models with multiple variables, and could only guarantee locally optimal solutions.

Considering these optimization efforts, Zink *et al.* (2009) and Trapp *et al.* (2011) illustrate the optimization of thermoacoustic systems, while taking into account thermal losses to the surroundings that are typically disregarded. Mathematical analysis and optimization is used to illustrate the conflicting nature of objective component considered in their modelling approach. In spite of the introductory nature of their works with respect of their plans to expand it and include a driven thermoacoustic refrigerators, the presented works are important contributions to thermoacoustics, as it merges the theoretical optimization approach with thermal investigation in thermoacoustics. Therefore, as several conflicting objectives have been identified, an effort to effectively implement the epsilon-constraint method for producing the Pareto optimal solutions in a multi-objective optimization mathematical programming method is carried out in this paper. This has been implemented in the widely used modelling language general algebraic modelling system (GAMS) (General Algebraic Modelling System, www.gams.com). As a result, GAMS codes are written to define, to analyse, and solve optimization problems to generate sets of Pareto optimal solutions unlike previous studies.

The remainder of this paper is organized in the following fashion: in Section 2, the modelling approach is presented. The fundamental components of the mathematical model characterizing the standing wave thermoacoustic heat engine are presented in Section 3. Section 4 describes the solution methodology of the multi-objective mathematical programming (MMP) problem. In Section 5, an illustration of the proposed approach is considered for a thermoacoustic couple (TAC). Section 6 concludes and presents all the results found in Appendix.

2. Modelling approach

In this section, the modelling approach for the physical standing wave engine depicted in Figure 2 is discussed; the development of the mathematical model and its corresponding optimization is included in Sections 3 and 4.

2.1 Simplification of thermoacoustic regenerator model

The optimization problem is reduced to a two-dimensional domain because of the symmetry present in the stack. Two constant temperature boundaries are considered,

namely, one convective boundary and one adiabatic boundary, as shown in Figure 3. For this model, only the regenerator geometry is considered; the model considers variation in operating condition and the interdependency of stack location and geometry.

Five different parameters are considered to characterize the regenerator:

(1) *L*: Stack length.

(2) *H*: Stack height.

(3) *Za*: Stack placement (with Za = 0 corresponding to the closed end of the resonator tube).

(4) Stack spacing.

(5) *N*: Number of channels.

Those parameters have been allowed to vary simultaneously.

2.2 Objectives

Five different objectives, as described by Trapp *et al.* (2011), namely, two acoustic objectives (acoustic work W of the thermoacoustic engine and viscous resistance R_V through the regenerator) and three thermal objectives (convective heat flow Q_{conv}, radiative heat flow Q_{rad} and conductive heat flow Q_{cond}) are considered to measure the quality of a given set of variable value that satisfies all of the constraints. Because work is the only objective to be maximized, its negative magnitude will be minimized along with all of the other components. Ultimately, optimizing the resulting problem generates optimal objective function value $G^* = [W^*, R_V^* Q_{conv}^*, Q_{rad}^*, Q_{cond}^*]$ and optimal solution $x^* = [L^*, H^*, d^*, Za^*, N^*]$.

As the five objectives are conflicting in nature (Trapp *et al.*, 2011), a multi-objective optimization approach has been used. The ultimate goal of the multi-objective optimization problem is to simultaneously maximize (or minimize) objective functions. As some of the objective functions conflict with each other, there is no exactly one solution but alternative solutions. Such potential solutions which cannot improve all the objective functions simultaneously are called efficient (Pareto optimal) solutions (Miettinen, 1999).

According to Hwang and Masud (1979), the methods for solving MMP problems can be classified into three categories, based on the phase in which the decision-maker involves in the decision-making process expressing his/her preferences: the a priori methods, the interactive methods and the a posteriori or generation methods. The a posteriori (or generation) methods give the whole picture (i.e. the Pareto set) to the decision-maker, before his/her final choice, reinforcing thus, his/her confidence to the final decision. In general, the most widely used generation methods are the weighting method and the epsilon-constraint method. These methods can provide a representative subset of the Pareto set which in most cases is adequate. The basic step towards further penetration of the generation methods in the multi-objective mathematical problems is to provide appropriate codes in a GAMS environment and produce efficient solutions.

3. Illustration of the optimization procedure of the regenerator

3.1 Boundary conditions

The five variables L, H, d, Za, N may only take values within the certain lower and upper bounds. The feasible domains for a thermoacoustic regenerator are defined as follows:

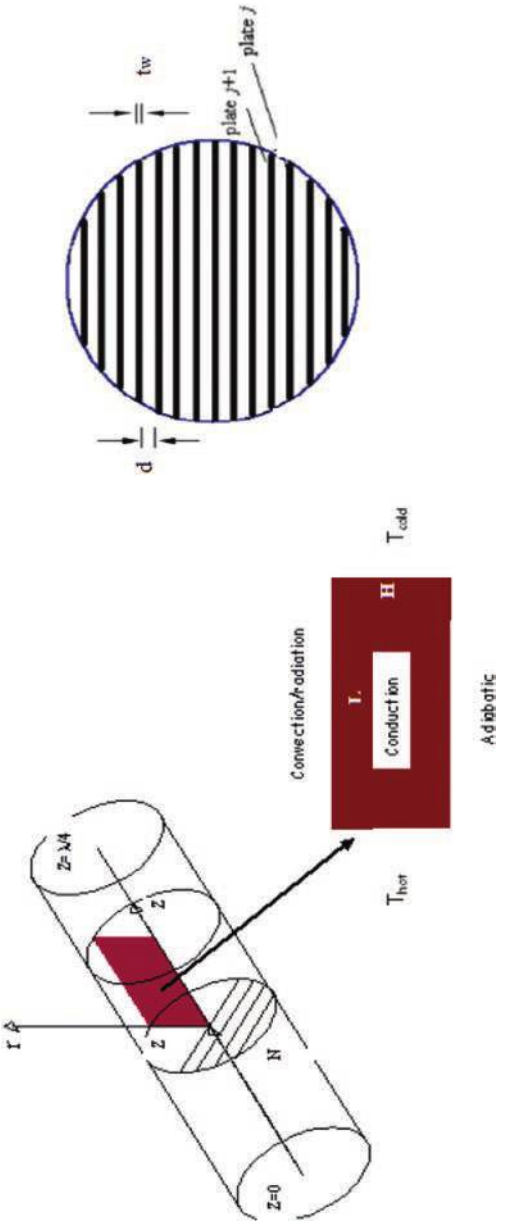

Figure 3.
Computational domain

$$\begin{aligned} L_{min} \le L \le L_{max} \\ H_{min} \le H \le H_{max} \\ d_{min} \le d \le d_{max} \\ Za_{min} \le Za \le Za_{max} - L \\ N_{min} \le N \le N_{max} \end{aligned} \quad (1)$$

$L, H, d, Za \in \Re +$ and $N \in Z +$

with:

$$d_{min} = 2\delta_k \text{ and } d_{max} = 4\delta_k \text{ (Tijani } \textit{et al.,} \text{ 2002)} \quad (2)$$

Additionally, the total number of channels N of a given diameter d is limited by the cross-sectional radius of the resonance tube H. Therefore, the following constraint relation can be determined:

$$N(d + t_w) \le 2H \quad (3)$$

where t_w represents the wall thickness around a single channel, and N_{min} and N_{max} predetermined values corresponding, respectively, to H_{min} and H_{max}.

The thermal penetration depth δ_k, the viscous penetration depth δ_v and the critical temperature are given by the following equations:

$$\delta_k = \sqrt{\frac{2K}{\rho_m c_p \omega}} \quad (4)$$

$$\delta_V = \sqrt{\frac{2\mu}{\rho_m \omega}} \quad (5)$$

$$\nabla T_{crit.} = \frac{\omega p_1^s}{\rho_m c_p u_1^s} \quad (6)$$

with K being the thermal conductivity, ρ_m the mean density, c_p the constant pressure specific heat, μ is the diffusivity of the working fluid and ω the angular frequency.

The following boundary conditions must also be enforced:

- Constant hot side temperature (T_h);
- Constant cold side temperature (T_C);
- Adiabatic boundary, modelling the central axis of the cylindrical stack:

$$\left.\frac{\partial T}{\partial r}\right|_{r=0} = 0 \quad (7)$$

- Free convection and radiation to surroundings (at T_∞) with temperature-dependent heat transfer coefficient (h), emissivity ε and thermal conductivity (k):

$$k\frac{\partial T}{\partial r}\Big|_{r=H} = h(T_S - T_\infty) + \varepsilon k_b(T_S^4 - T_\infty^4) \tag{8}$$

3.2 Acoustic power

The acoustic power per channel has been derived by Swift (2002). The following equation can be derived for N channel:

$$W = \omega LN\left(\frac{\pi H^2}{2(d + t_w)}\right)\left[\delta_k\frac{(\gamma - 1)p^2}{\rho c^2(1 + \varepsilon)}(\nabla T_{crit.} - 1) - \delta_v \rho u^2\right] \tag{9}$$

The relation between the stack perimeter Π and the cross-sectional area A, as determined by Swift (2002) is given by:

$$\Pi = \frac{2A}{d + t_w} \tag{10}$$

The amplitudes of the dynamic pressure p and gas velocity u due to the standing wave in the tube are given by:

$$p = p_{max}\cos\left(\frac{2\pi Za}{\lambda}\right) \tag{11}$$

$$u = u_{max}\sin\left(\frac{2\pi Za}{\lambda}\right) \tag{12}$$

with

$$u_{max} = \frac{p_{max}}{\rho c} \tag{13}$$

The heat capacity ratio can be expressed by (Zink *et al.*, 2009):

$$\varepsilon = \frac{(\rho c_p \delta_k)_g}{(\rho c_p \delta_s)_s}\frac{\tanh((i + 1)y_0/\delta_k)}{\tanh((i + 1)l/\delta_s)} \tag{14}$$

This expression can be simplified to values of $\varepsilon = y_0/\delta_k$ if $y_0/\delta_k < 1$ and $\varepsilon = 1$ if $y_0/\delta_k > 1$ (Zink *et al.*, 2009), where y_0 half of the channel height is, l is half of the wall thickness and δ_s is the solid's thermal penetration depth.

3.3 Viscous resistance

Just as the total acoustic power of the stack was dependent on the total number of channels, the viscous resistance also depends on this value. The following equation can be derived (Swift, 2002):

$$R_V = \frac{\mu\Pi L}{A_C^2\delta_V N} = \frac{2\mu}{\delta_V}\frac{L}{(d + t_w)\pi H^2 N} \tag{15}$$

3.4 Convective heat flux

The mechanism of convection for the thermoacoustic devices in this study is free convection with air at room temperature. The rate of heat transfer (Long, 1999), $\dot{Q}_{conv}$ to surround air due to convection is:

$$\dot{Q}_{conv} = hA(T_S - T_\infty) \tag{16}$$

The heat transfer coefficient h and the heat flux to the surroundings were estimated using a linear temperature profile. In this model, the actual temperature distribution throughout the stack is taken into account by utilizing MATLAB finite element toolbox (The Mathworks, 2007), which captures the temperature dependence of the heat transfer coefficient. Only the temperature distribution at the shell surface and the temperature gradient at the cold side are of interest. Trapp *et al.* (2011) have derived the final surface temperature distribution as a function of axial direction Za. It is given by:

$$T_S = T_h e^{\ln\left(\frac{T_C}{T_h}\right)\frac{Za}{L}} \tag{17}$$

The convective heat transfer coefficient and the radiative heat flux to the surroundings are assumed to be dependent on this temperature. The total convective heat transfer across the cylindrical shell in its integral form can be described by:

$$Q_{conv} = H\int_0^{2\pi}\int_0^{L} h(T(z))(T(z) - T_\infty)dzd\rho \tag{18}$$

For the case of a horizontal tube subject to free convection (Baehr and Stephan, 2004), the heat transfer coefficient h is derived from the Nusselt number, which is a non-dimensional heat transfer coefficient as follows:

$$h(Ts) = \frac{k_g}{2H}Nu \tag{19}$$

$$Nu = 0.36 + \frac{0.518Ra_D^{\frac{1}{4}}}{\left[1 + \left(\frac{0.559}{Pr}\right)^{\frac{9}{16}}\right]^{\frac{4}{9}}} \tag{20}$$

This expression depends on the Prandtl number, which can be expressed by:

$$Pr = \frac{\nu}{\alpha} \tag{21}$$

$$Ra = \frac{g\beta(T_S - T_\infty)8H^3}{\nu\alpha} \tag{22}$$

where Pr is the Prandtl number, T_S is the surface temperature, T_∞ is the (constant) temperature of the surroundings, ν is the viscosity of the surrounding gas and α is the thermal diffusivity of the surrounding gas (air). The temperature distribution stated in equation (17) is then used to determine the convective heat transfer to the surroundings. After integrating, the following heat flow expression is derived:

$$Q_{conv} = 2\pi HLh\left[\frac{T_C - T_H}{\ln\left(\frac{T_C}{T_H}\right)} - T_\infty\right] \tag{23}$$

The following constraint can be derived from equation (20) and equation (22):

$$Za \geq L\log\left(\frac{T_{inf}}{T_C}\right) \tag{24}$$

3.5 Radiative heat flux

For an object having a surface area, A, a temperature, T, surrounded by air at temperature T_∞, the object will radiate heat at a rate, $\dot{Q}_{rad}$ (Seaway, 1996):

$$\dot{Q}_{rad} = k_B \varepsilon A(T^4 - T_\infty^4) \tag{25}$$

The radiation heat flux becomes increasingly important as T_H increases, as shown in the following equation:

$$Q_{rad} = HK_B \int_0^{2\pi}\int_0^L \varepsilon(T_{(z)}{}^4 - T_\infty^4)dzd\rho \tag{26}$$

where k_B is the Stefan–Boltzmann constant, and ε is the surface emissivity, which depends on the emitted wavelength and in turn is a function of temperature. After integrating, the following heat flow expression is derived:

$$Q_{rad} = 2\pi HLk_B\varepsilon\left[\frac{T_C^4 - T_H^4}{4\ln\left(\frac{T_C}{T_H}\right)} - T_\infty^4\right] \tag{27}$$

3.6 Conductive heat flux

The temperature distribution is used to determine the temperature gradient at the top surface Za, r = H. According to Fourier's law (Long, 1999), the heat flow, $\dot{Q}_{cond}$ in the z direction, through a material is expressed as:

$$\frac{\Delta Q}{\Delta t} = -kA\frac{\Delta T}{\Delta x} \tag{28}$$

The rate at which the flow of heat occurs depends on the material, the geometry and the temperature gradient; it is specified by its conductivity. Similar to the cylindrical shell, this heat flux has to be integrated over the whole surface representing the cold side:

$$Q_{cond} = \int_0^{2\pi} \int_0^{H} \left(k_{zz} \frac{\partial T}{\partial r}\right) dr d\rho \tag{29}$$

Where the value of the axial thermal conductivity k_{zz} is determined by the following equation (Zink *et al.*, 2009):

$$k_{zz} = \frac{k_S t_w + k_g d}{t_w + d} \tag{30}$$

Therefore:

$$\left.\frac{\partial T}{\partial z}\right|_{z=L} = \frac{\ln\left(\frac{T_C}{T_H}\right)\left(\frac{T_C}{T_H}\right)}{L} \tag{31}$$

And after integration:

$$Q_{cond} = \frac{k_{zz}}{L} \pi H^2 T_C \ln\left(\frac{T_H}{T_C}\right) \tag{32}$$

4. Solution methodology of the MMP problem

All the expressions involved in the MMP have been presented in the previous section. The optimization task is formulated as a five-criteria mixed-integer non-linear programming problem that simultaneously minimizes the negative magnitude of the Acoustic Work W (as it is the only objective to be maximized), the viscous resistance R_V, the convective heat flux Q_{conv}, the radiative heat flux Q_{rad} and the conductive heat flux Q_{conv}:

$$(\text{MPF}) \min_{L,H,Z_a,d,N} \xi = \left\{-W_{(L,H,Z_a,d,N)}, R_{V(L,H,Z_a,d,N)}, Q_{conv(L,H,Z_a,d,N)}, Q_{rad(L,H,Z_a,d,N)}, Q_{cond(L,H,Z_a,d,N)}\right\} \tag{33}$$

Subject to the constrains described by equations (1), (2), (3) and (24).

In this formulation, (L, H, Z_a, d, N) denotes the geometric parameters.

There is no single optimal solution that simultaneously optimizes all the five objectives functions. In these cases, the decision-makers are looking for the "most preferred" solution. To find the most preferred solution of this multi-objective model, the augmented epsilon-constraint method (AUGMECON) as proposed by Mavrotas (2009) is applied. The AUGMECON method has been coded in GAMS. The code is available in the GAMS library (www.gams.com/modlib/libhtml/epscm.htm) with an example. While the part of the code that has to do with the example (the specific objective functions and

constraints), as well as the parameters of AUGMENCON have been modified in this case, the part of the code that performs the calculation of payoff table with lexicographic optimization and the production of the Pareto optimal solutions is fully parameterized to be ready to use.

Practically, the epsilon-constraint method is applied as follows: from the payoff table the range of each one of the p-1 objective functions that are going to be used as constraints is obtained. Then the range of the i-th objective function to qi equal intervals using $(q_i - 1)$ intermediate equidistant grid points is divided. Thus in total $(q_i + 1)$ grid points that are used to vary parametrically the right hand side (e_i) of the i-th objective function is obtained. The total number of runs becomes $(q_2 + 1) \times (q_3 + 1) \times [\ldots] \times (q_p + 1)$. The epsilon-constraint method has several important advantages over traditional weighted method. These advantages are listed by Mavrotas (2009). In the conventional epsilon-constraint method, there is no guarantee that the obtained solutions from the individual optimization of the objective functions are Pareto optima or efficient solutions. To overcome this deficiency, the lexicographic optimization for each objective functions to construct the payoff table for the MMP is proposed to yield only Pareto optimal solutions (it avoids the generation of weakly efficient solutions) (Aghaei *et al.*, 2009). The mathematical details of computing payoff table for MMP problem can be found by Aghaei *et al.* (2009). The augmented epsilon-constraint method for solving model [equation (33) can be formulated as follows (more details can be found by Mavrotas (2009) and Aghaei *et al.* (2009)]:

$$\max\left(W_{(L,H,Z_a,d,N)} + \mathrm{dir}_1\, r_1 \times \left(\frac{s_2}{r_2} + \frac{s_3}{r_3} + \frac{s_4}{r_4} + \frac{s_5}{r_5}\right)\right)$$

$$\text{s.t. } R_{V(L,H,Z_a,d,N)} - \mathrm{dir}_2\, s_2 = e_2 \tag{34}$$

$$Q_{\mathrm{conv}(L,H,Z_A,d,N)} - \mathrm{dir}_3\, s_3 = e_3$$

$$Q_{\mathrm{rad}(L,H,Z_A,d,N)} - \mathrm{dir}_4\, s_4 = e_4$$

$$Q_{\mathrm{conv}(L,H,Z_A,d,N)} - \mathrm{dir}_5\, s_5 = e_5$$

$$s_i \in \Re^+$$

Where dir_i is the direction of the i-th objective function, which is equal to -1 when the i-th function should be minimized, and equal to $+1$, when it should be maximized. Efficient solutions of the problem are obtained by parametrical iterative variations in the e_i. s_i are the introduced surplus variables for the constraints of the MMP problem. $r_i s_i / r_i$ is used in the second term of the objective function, to avoid any scaling problem. The formulation of equation (34) is known as the augmented epsilon-constraint method due to the augmentation of the objective function W by the second term.

5. Case study

To illustrate this approach, a TAC, as described by Atchley *et al.* (1990), is considered. It consists of a parallel-plate stack placed in helium-filled resonator. All relevant parameters are given in Tables I and II.

Table I. Specifications for thermoacoustic couple

Parameter	Symbol	Value	Unit
Isentropic coefficient	ν	1.67	
Gas density	ρ	0.16674	kg/m^3
Specific heat capacity	c_p	51,93.1	J/kg.K
Dynamic viscosity	μ	$1.9561.10^{-5}$	kg/m.s
Maximum velocity	u_{max}	670	m/s
Maximum pressure	p_{max}	1,14,003	Pa
Speed of sound	c	1,020	m/s
Thickness plate	t_w	1.91.10-4	m
Frequency	f	696	Hz
Thermal conductivity helium	k_g	0.16	W/(m.K)
Thermal conductivity stainless steel	k_s	11.8	W/(m.K)
Isobaric specific heat capacity	c_p	5193.1	J/(kg.K)

Table II. Additional parameters used for programming

Parameter	Symbol	Value	Unit
Temperature of the surrounding	T_∞	298	K
Constant cold side temperature	T_c	300	K
Constant hot side temperature	T_H	700	K
Wavelength	λ	1.466	m
Thermal expansion	β		1/K
Thermal diffusivity	α	2.1117E-5	m^2s-1

The following constraints (upper and lower bounds) have been enforced on variables for the solver to carry out the search of the optimal solutions in those ranges:

$$\begin{aligned} &L.lo = 0.005; L.up = 0.05; \\ &Za.lo = 0.005; \\ &H.lo = 0.005; \\ &d.lo > 2.\delta_k; d.up < 4.\delta_k \end{aligned} \tag{35}$$

A lexicographic optimization for the payoff table is used; the application of model equation (34) will provide only the Pareto optimal solutions, avoiding the weakly Pareto optimal solutions. Efficient solutions of the proposed model have been found using AUGMENCON method and the LINDOGLOBAL solver. To save computational time, the early exit from the loops as proposed by Mavrotas (2009) has been applied. Additionally, a desirable characteristic of the epsilon-constraint method is that you can control the density of the efficient set representation by properly assigning the value of grid point. The higher the number of grid point, the more dense is the representation of the efficient set but with the cost of higher computation time. The range of each five objective functions is divided in four intervals (five grid points). The integer variable N has been given values of 20 to 50. This process generates optimal solutions corresponding to each integer variable. The computation time for five grid points per objective function varied from 3,061.938 seconds (for $N = 40$) to 15,544.188 seconds (for $N = 45$) in a Pentium IV 1.6

GHz computer. Optimal solutions have been found for $N = 26$, $N = 31$, $N = 33$, $N = 36$, $N = 38$, $N = 39$, $N = 40$, $N = 42$, $N = 43$, $N = 45$ and $N = 49$. The following section report only five sets of Pareto solutions obtained.

Figure 4 represents the Pareto solutions graphically; it shows that there is not only a single optimal solution that optimizes the geometry of the regenerator. More results can be found in Appendix (Figure 5 and Figures A1-A10). To produce as much acoustic power W as possible and minimize viscous resistance and thermal losses simultaneously, there is a specific stack length L to which correspond a specific stack height H, a specific stack position Za, a specific stack spacing d and a specific number of channels N. This study highlights the fact that the geometrical parameters are interdependent, which support the use of a multi-objective approach for optimization. It should be noted that in all cases that locating the stack closer to the closed end produce the desirable effect. All Pareto optimal solutions can be identified to reinforce the decision-maker final decision and choice.

These optimal solutions are then used to construct Figure 5 and Figures A11-A14 representing, respectively, acoustic work, viscous resistance, conductive, convective and radiative heat fluxes. Five different solutions corresponding to the

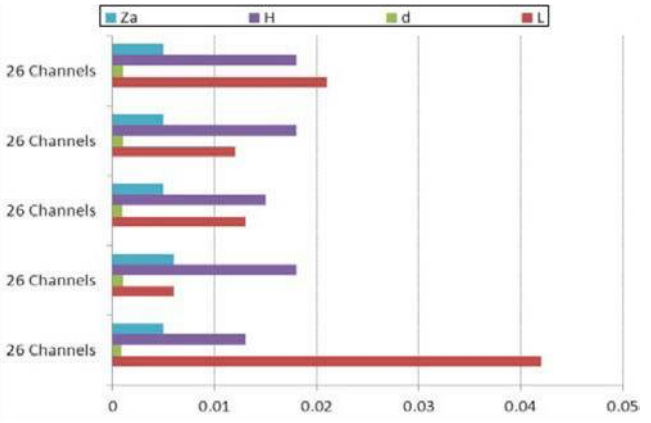

Figure 4.
Optimal structural variables for $N = 26$

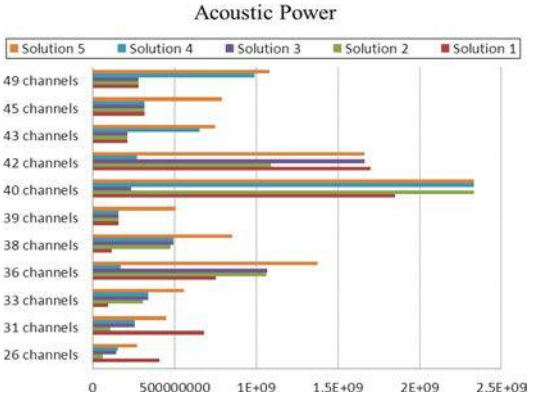

Figure 5.
Acoustic power function of N describing five solutions set

optimal solutions generated in Figures 4 and 5 and A6-A10 are presented. Considering the decision-maker preference, these figures (Figure 5 and Figures A11-A14) are good indications of expected objective functions values for specific geometrical parameters. While maximum value is expected for $N = 40$ for the acoustic work, minimal values of viscous resistance, conductive heat flux, convective heat flux and radiative for $N = 49$ (Figure A11), $N = 26$ (Figure A12), $N = 39$ (Figure A13) and $N = 39$ (Figure A14) are expected. The conflicting nature of the five objectives can be observed in these profiles.

6. Conclusion

In order for a thermoacoustic engines to be competitive on the current market, optimization should be performed to improve their overall performance. Previous studies have relied heavily upon parametric studies. This work targets the geometry of the thermoacoustic regenerator and uses multi-objective optimization approach to find the optimal set of geometrical parameters that optimizes the device. Five different parameters (stack length, stack height, stack placement, stack spacing and number of channels) describing the geometry of the device have been studied. Five different objectives have been identified; a non-linear multi-objective programming approach for thermoacoustic regenerator has been implemented in GAMS. To avoid weakly efficient point, a payoff table from the lexicographic optimization is used. An improved version of a multi-objective solution method, i.e. the epsilon-constraint method called augmented epsilon-constraint method (AUGMENCON) is applied. To illustrate this approach, five efficient solutions that optimize the regenerator geometry have been computed; in each case, the acoustic power, the viscous resistance and the thermal losses have been determined. The lexicographic optimization provides a much more dense representation of the efficient set and more meaningful results. The geometrical parameters of the regenerator have been found to be interdependent which support the use of this multi-objective approach to optimize the geometry of thermoacoustic engine.

References

Aghaei, J. Amjady, N. and Shayanfar, H.A. (2009), "Multi-objective electricity market clearing considering dynamic security by lexicographic optimization and augmented epsilon constraint method", *Applied Soft Computing*, Vol. 11 No. 4, pp. 3846-3858.

Atchley, A., Hofler, A., Muzzerall, T., Kite, M.L. and Chianing, A.O. (1990), "Acoustically generated temperature gradients in short plates", *Journal of Acoustical Society of America*, Vol. 88 No. 1, p. 251.

Backhaus, S. and Swift, G.W. (2000), "A thermoacoustic stirling heat engine: detailed study", *Journal of the Acoustical Society of America*, Vol. 107 No. 6, pp. 3148-3166.

Baehr, H.D. and Stephan, K. (2004), *Wärme – und Stoffübertragung: transl: Heat and Mass Transfer*, 4th ed., Springer, Heidelberg.

Bastyr, K.J. and Keolian, R.M. (2003), "High-frequency thermoacoustic Stirling heat engine demonstration device", *Acoustics Research Letters Online*, Vol. 4 No. 2, pp. 37-40.

Besnoin, E. (2001), "Numerical study of thermoacoustic heat exchangers", PhD thesis, Johns Hopkins University, Maryland.

Generalized Algebraic modelling Systems (GAMS), available at: www.gams.com

Hwang, C.L. and Masud, A. (1979), "Multiple objective decision making: methods and applications: a state of the art survey", Lecture Notes in Economics and Mathematical Systems Vol. 164, Springer-Verlag, Berlin.

Long, C. (1999), "Essential heat transfer", *Longman Essex*, Longman, London, p. 5, p. 173, pp. 175-181, p. 184, p. 84.

Mavrotas, G. (2009), "Effective implementation of the ε-constraint method in multiobjective mathematical programming problems", *Applied Mathematics and Computation*, Vol. 213 No. 2, pp. 455-465.

Miettinen, K. (1999), *Nonlinear Multiobjective Optimization*, Springer, Heidelberg.

Minner, B.L., Braun, J.E. and Mongeau, L.G. (1997), "Theoretical evaluation of the optimal performance of a thermoacoustic refrigerator", *ASHRAE Transactions Proceedings of the Winter Meetings*, Vol. 103 No. 1, pp. 873-887.

Poese, M.E., Smith, R.W., Garrett, S.L., Van Gerwen, R.V. and Gosselin, P. (2004), "Thermoacoustic refrigeration for ice cream sales", Proceedings of the 6th IIR Gustav Lorentzen Conference, Glasgow.

Seaway, R.A. (1996), *Physics for Scientist and Engineers with Modern Physics*, 4th ed, College Publishing, Philadelphia.

Swift, G.W. (1988), "Thermoacoustic engines", *The Journal of the Acoustical Society of America*, US Patent No. 6,032,464, Vol. 4 No. 1, pp. 1146-1180.

Swift, G.W. (2002), *Thermoacoustics: A Unifying Perspective for Some Engines and Refrigerators*, Acoustical society of America, Melville, New York, NY.

Swift, G.W., Backhaus, S.N. and Gardner, D.L. (2000), "Traveling-wave Device with Mass Flux Suppression", US Patent No. 6032464.

The MathWorks (2007), *MATLAB User's Guide*, The Math Works, Natick, Massachusetts.

Tijani, M.E.H., Zeegers, J.C.H. and De Waele, A.T.A.M. (2002), "The optimal stack spacing for thermoacoustic refrigeration", *Journal of the Acoustical Society of America*, Vol. 112 No. 1, pp. 128-133.

Trapp, A.C., Zink, F. Prokopyev, O.A. and Schaefer, L. (2011), "Thermoacoustic heat engine modelling and design optimization", *Journal of Applied Thermal Engineering*, Vol. 31 Nos 14/15, pp. 2518-2528.

Wetzel, M. and Herman, C. (1997), "Design optimization of thermoacoustic refrigerators", *International Journal of Refrigeration*, Vol. 20 No. 1, pp. 3-21.

Wheatley, J.C., Hofler, T., Swift, G.W. and Migliori, A. (1985), "Understanding some simple phenomena in thermoacoustics with applications to acoustical heat engines", *American Journal of Physics*, Vol. 53 No. 2, pp. 147-162.

Zink, F. Waterer, H. Archer, R. and Schaefer, L. (2009), "Geometric optimization of a thermoacoustic regenerator", *International Journal of Thermal Sciences*, Vol. 48 No. 12, pp. 2309-2322.

Appendix

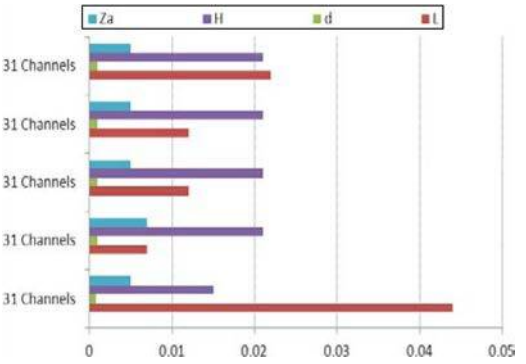

Figure A1.
Optimal structural variables for $N = 31$

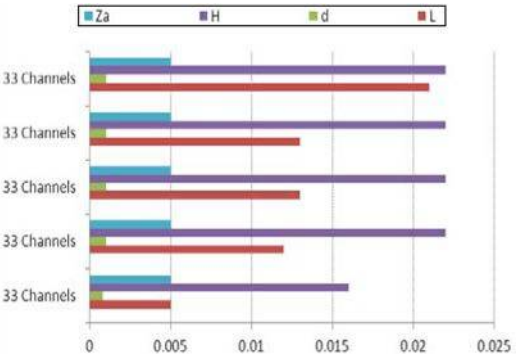

Figure A2.
Optimal structural variables for $N = 33$

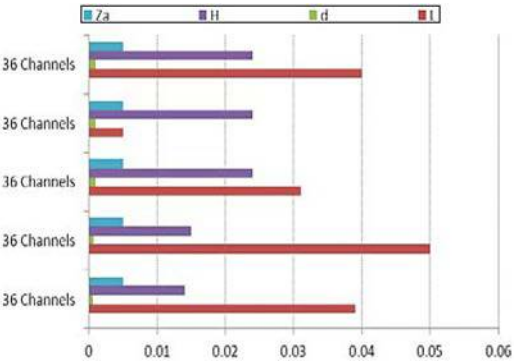

Figure A3.
Optimal structural variables for $N = 36$

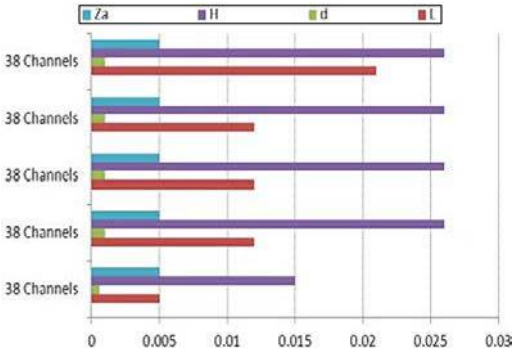

Figure A4.
Optimal structural variables for $N = 38$

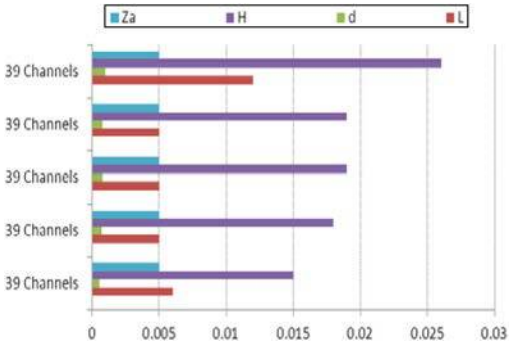

Figure A5.
Optimal structural variable for $N = 39$

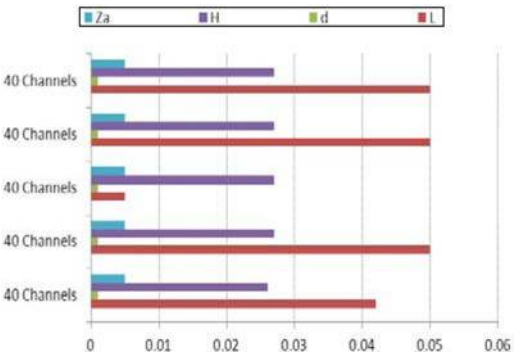

Figure A6.
Optimal structural variable for $N = 40$

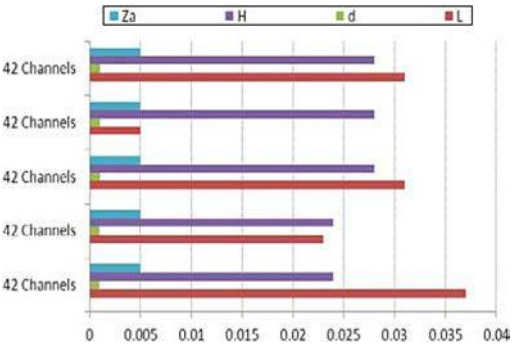

Figure A7.
Optimal structural variable for $N = 42$

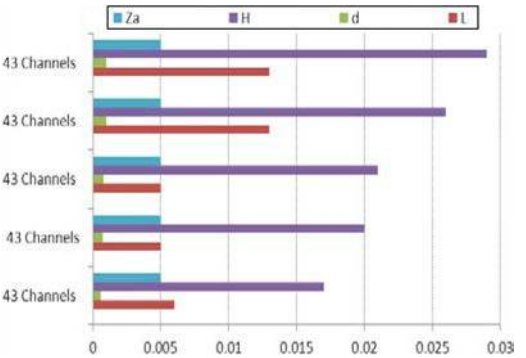

Figure A8.
Optimal structural variable for $N = 43$

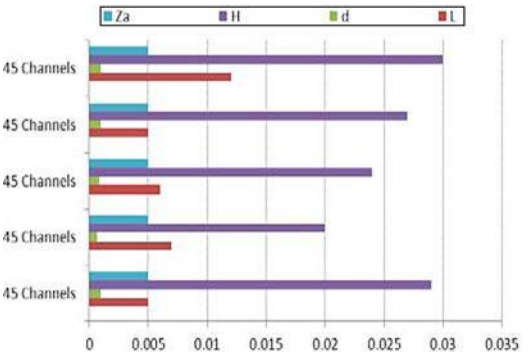

Figure A9.
Optimal structural variable for $N = 45$

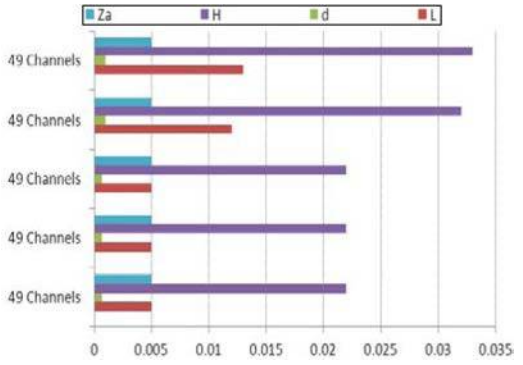

Figure A10.
Optimal structural variable for $N = 49$

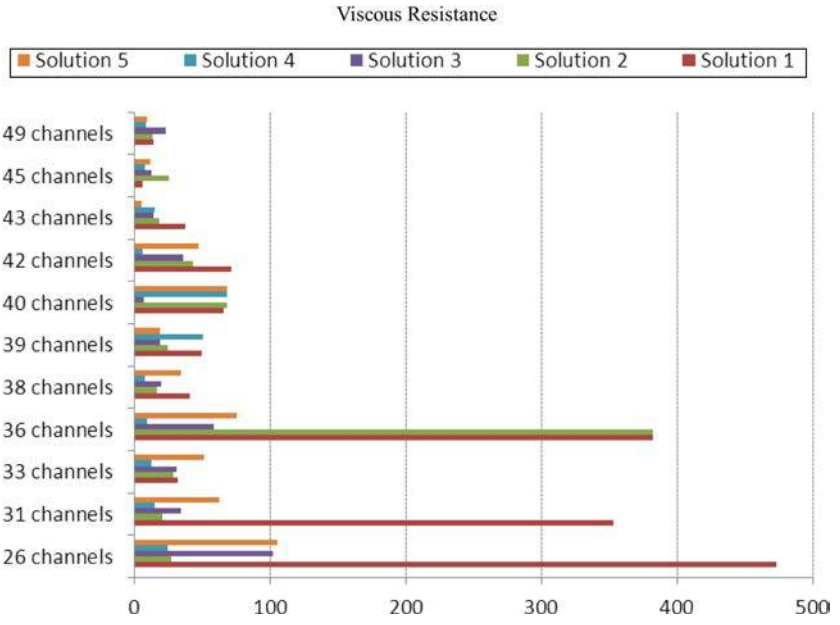

Figure A11.
Viscous resistance function of N representing five solutions set

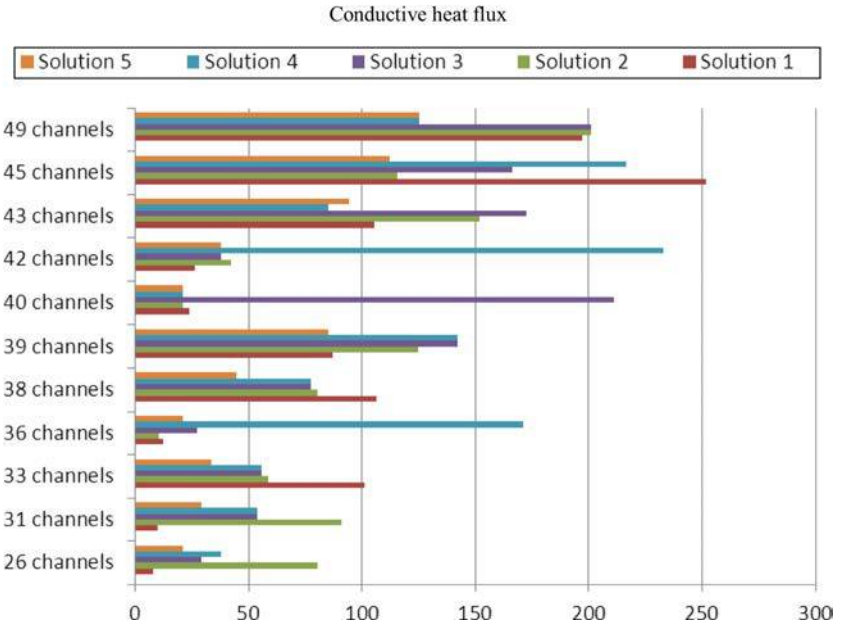

Figure A12.
Conductive heat flux function of N representing five solutions set

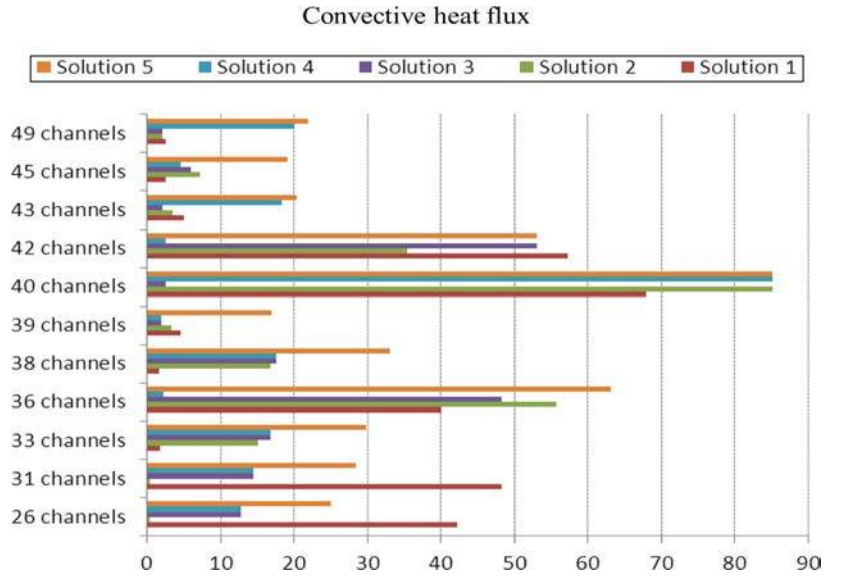

Figure A13.
Convective heat flux function of N representing five solutions set

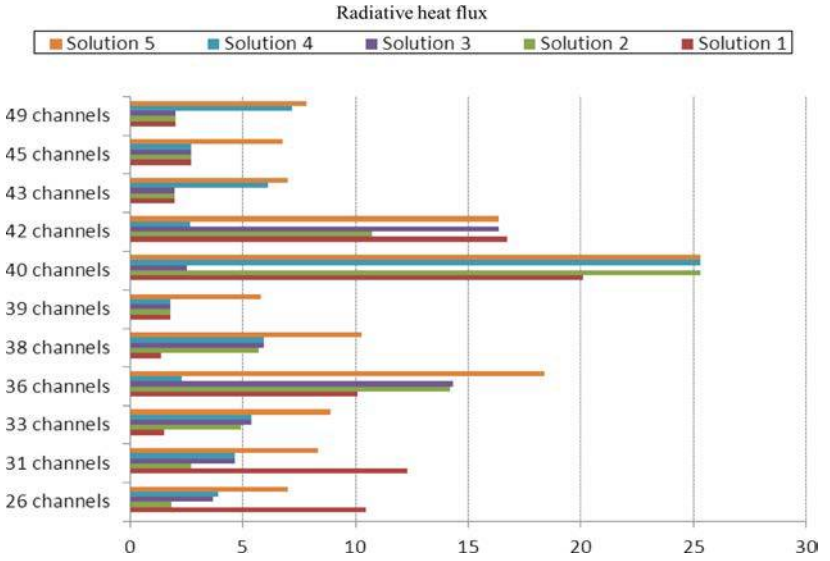

Figure A14.
Radiative heat flux function of N representing five solutions set

Corresponding author
L.K. Tartibu can be contacted at: lagougetartibu@yahoo.fr